Effect of Particle Volume Fraction on Crack-Tip Crazes in High Impact Poly(methyl Methacrylate)

O. MAUZAC and R. SCHIRRER, *Institut Charles Sadron (CRM-EAHP), 4 rue Boussingault, F-67000 Strasbourg, France*

Synopsis

The fracture behavior of a PMMA toughened by small (0.2 μm diameter) rubber particles was investigated over a wide range of rubber particle volume fractions. Crack tip morphology, material toughness, and fracture surfaces were studied. Whereas isolated particles have no effect, interactions between particles strongly modify the fracture behavior. Interactions occur via two different mechanisms: (i) an overlap of the stress enhancements due to particles, which is a function of the ratio of the distance between particles versus particle diameter; (ii) a geometrical "sifter" effect, which occurs when the distance between particles is less than the craze thickness.

INTRODUCTION

With regard to crack propagation, toughening of thermoplastics may involve various mechanisms depending on the structure of the rubbery phase in the polymer. For example, very small particles (less than 1 μm diameter) are supposed to enhance microshear band formation, whereas larger particles preferentially enhance multiple crazing in the amorphous matrix.[1-4] For the particle volume fraction effect, it is generally admitted that the stress enhancement of each spherical particle acts up to a distance of one particle radius around its surface,[5] and toughening is effective when the edge-to-edge distance between particles is less than one particle radius.[6-8]

Though materials with large particles (diameters greater than 1 μm) have been widely studied, the case of poly(methyl methacrylate) (PMMA) toughened with very small rubber particles (about 0.2 μm diameter) is much less known. Most authors agree with Donald and Kramer, who think that a small isolated particle cannot generate a craze.[9] Another particularity of this material is that the crack-tip craze is much larger than the particles, and it is not known whether particles can be "absorbed" by the craze or not.

Optical interferometry is known to be an efficient means to visualize the crack-tip morphology, especially in the case where a single craze exists at the crack tip, as in PMMA at room temperature.[10,11] Therefore, the propagating crack tip in a PMMA modified with very small rubber particles has been observed by means of optical interferometry over a wide range of particle volume fractions. Scanning electron microscopy (SEM) has also been used to study the fracture surfaces of the specimens that had been broken on the interferometry-tensile device.

Journal of Applied Polymer Science, Vol. 38, 2289–2302 (1989)
© 1989 John Wiley & Sons, Inc. CCC 0021-8995/89/122289-14$04.00

EXPERIMENTAL

Materials and Experimental Setup

The materials were supplied by NORSOLOR SA (CdF Chimie), and consisted of a set of dispersions of a latex (ref. M1) in a PMMA matrix (ref. 7H). The latex volume fractions (i.e., "total" particle volume fraction) ranged from 0.004% to 40%, by one-decade steps. Mixing was performed on a calender. Like any "mechanical" method, calendering is not likely to give perfectly homogeneous dispersions, especially when the dispersed volume fraction is less than a few percent. Nevertheless, the observed trends of the material's response versus latex content and the reproducibility of experimental results lead to the conclusion that the dispersion was fairly good over the whole range of volume fractions.

Small compact tension specimens were milled from 3.5 mm thick plates. These specimens were tested on a tensile device allowing the observation of the interference pattern at the crack tip. A complete description of the experimental setup will be found elsewhere.[11] All experiments were performed in air at room temperature (25°C). The cracks were initiated from machined precracks by fatigue under cyclic 200 Hz tensile loading, and subsequently slowly propagated under a static constant stress.

There are two main parameters that describe the dispersion of particles in a matrix: (i) the mean distance between two particles; (ii) the ratio of mean distance between particles vs. mean particle diameter. However, in the material studied here, both parameters are equivalent since the distribution of particle sizes is very narrow (emulsion polymerized latex), only the distance between particles follows a statistical distribution. In the analysis of experimental results it will be considered that particles are distributed at random, with the only limitation being that no particle overlap is allowed. As the particles have a core–shell structure (Fig. 1), only the rubbery core [13% PS, 87% poly(butyl acrylate)] will be taken into account: the shell (PMMA) may be considered to belong to the matrix from the mechanical point of view. For this reason the efficient particle volume fraction (v_p) is that corresponding not to the whole latex but to the rubbery cores. As the core to shell volume ratio inside a particle is $p = 1.86$, v_p is related to the latex (or "total particle")

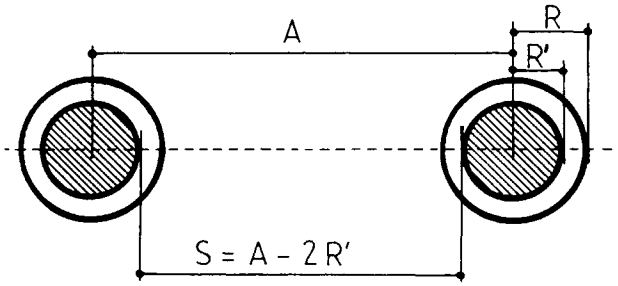

Fig. 1. Parameters describing the dispersion of core-shell emulsion particles in a PMMA matrix (core = rubber, shell = PMMA): R = radius of the core-shell particle; R' = radius of the rubbery core ("true" particle radius); A = center-to-center interparticle distance; S = edge-to-edge interparticle distance.

volume fraction v_L via

$$v_p = v_L p(1 + p)^{-1} = 0.65 v_L \tag{1}$$

The number N_0 of particles per unit volume is equal to the particle volume fraction divided by the volume of a particle:

$$N_0 = v_L(4\pi R^3/3)^{-1} = v_p(4\pi R'^3/3)^{-1} \tag{2}$$

where R and R' are the radii of the whole particle and of the rubbery core.

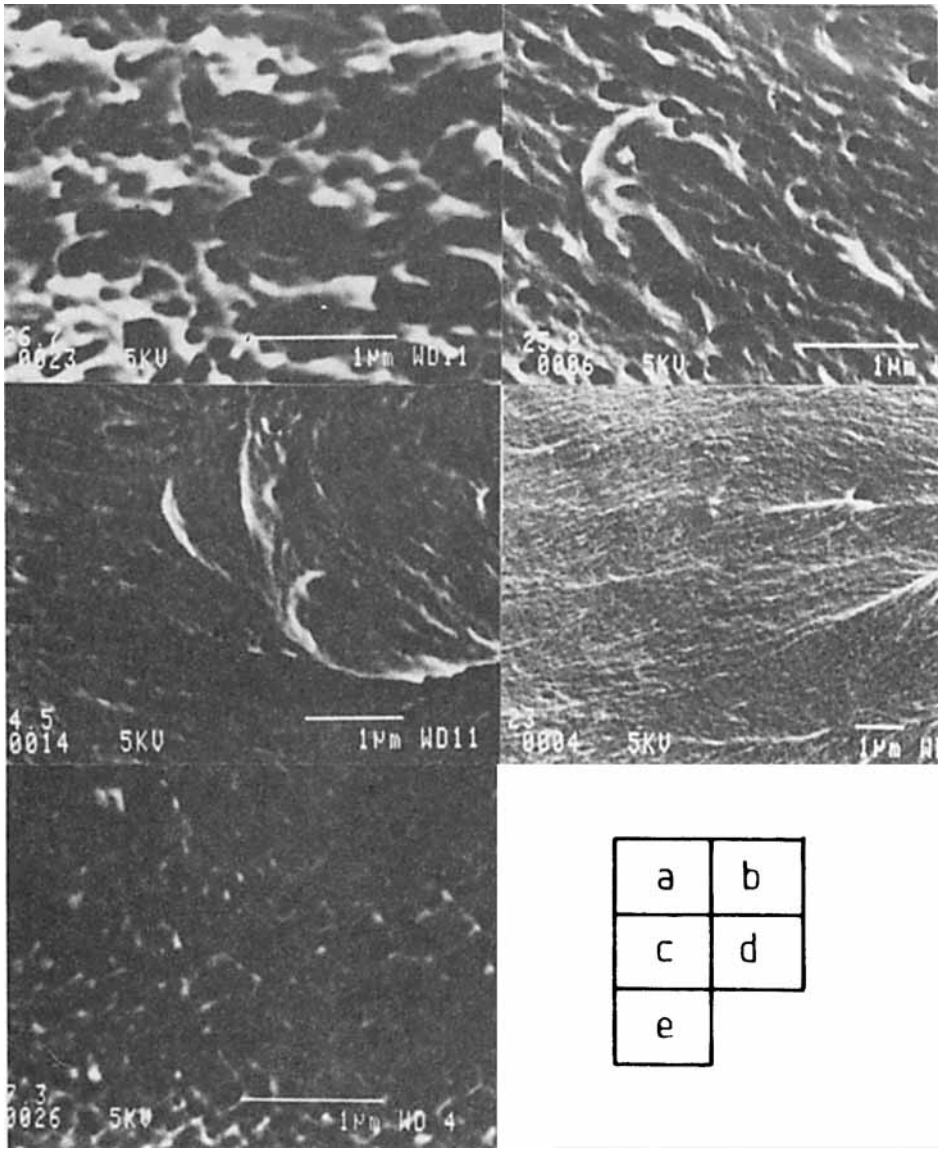

Fig. 2. SEM photographs of fracture surfaces for various particle volume fractions v_p (%): (a) 26; (b) 2.6; (c) 0.26; (d) 0.026; (e) 0.0026.

The mean distance $\langle A \rangle$ between centers of neighboring particles scales like

$$\langle A \rangle = (1/N_0)^{1/3} = 0.19 v_p^{-1/3} \tag{3}$$

(with $\langle A \rangle$ in μm, N_0 in μm^{-3}, v_p dimensionless, and $R' = 0.12$ μm).

RESULTS

SEM Studies of Fracture Surfaces

Typical photographs are shown in Figure 2 for the different materials. They show an increasing density of randomly distributed markings of about 0.2 μm diameter (which is nearly the particle diameter) with increasing particle volume fraction. These patterns are remarkably reproducible. For the lowest particle volume fraction ($v_p = 0.0026\%$) markings can hardly be found even over large areas [Fig. 2(e)]. The surface appears smooth when observed at moderate magnification ($\times 500$) and broken craze fibrils can be seen at higher magnification ($\times 30{,}000$) as in the case of pure PMMA.[12] Conversely, for the highest particle volume fraction ($v_p = 26\%$), the whole surface consists of contiguous markings, its appearance comparing with that of a sponge. The large thickness of the whitened zone (about 0.5 mm) suggests that the sponge-like structure probably extends deep below the surface.

Quantitative results (Table 1) will be given as follows: for each particle volume fraction the number ρ_{SEM} of markings per unit surface has been measured on many photographs (yet ρ_{SEM} does not have a clean statistical meaning when the number of markings is very low). Note that ρ_{SEM} is related to the mean distance $\langle \lambda_{SEM} \rangle$ between neighbor markings via

$$\langle \lambda_{SEM} \rangle = \rho_{SEM}^{-1/2} \tag{4}$$

TABLE I
Experimental[a] and Calculated Results[b]

v_p (%)	ρ_{SEM} (μm^{-2})	Φ_{INT}	K_{1c} (MPa $m^{1/2}$)	ρ_1 (μm^{-2})	Φ_2
0.0026	$\ll 0.02$	None	0.86–0.90	0.006	0.0004
0.026	0.02–0.08	None	0.84–0.92	0.06	0.04
0.26	0.59–0.64	1–5	0.81–0.91	0.59	4
2.6	2.8–5.2	Craze bundles	1.06–1.17	5.9	400
26	13–19	Craze bundles	1.17–1.36	59	40,000

[a] ρ_{SEM} = density of markings on the fracture surface (from SEM pictures); Φ_{INT} = number of perturbations of the interference fringe pattern that are visible in the field of the optical microscope (0.2 mm^2); K_{1c} = stress intensity factor during the propagation (10 μm/s) of the crack-tip craze.

[b] ρ_1 = theoretical value for ρ_{SEM} assuming that each particle absorbed by the craze leaves a marking on the fracture surface; Φ_2 = theoretical value for Φ_{INT} calculated by means of the "sifter effect" model.

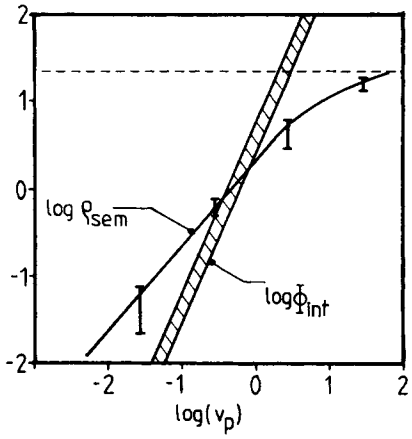

Fig. 3. ρ = density of markings on the fracture surface versus the particle volume fraction: (scatter bars) ρ_{SEM}, experimental data; (—) ρ_1, fit of experimental data by the model in the Discussion (the slope of the line in the log–log plot is 1); (- - -) saturation effect with ρ_{MAX} = 22 μm^{-2}. Φ_{INT} = number of perturbations of the interference fringe pattern vs. v_p; the slope in the log–log plot is about 2.

Experimental values of ρ_{SEM} have been plotted vs. v_p on Figure 3, yielding the experimental scaling law: ρ_{SEM} is proportional to v_p except for the highest volume fraction (v_p = 26%). The latter discrepancy can be explained by the saturation of ρ_{SEM}. The highest value for ρ_{SEM} that can be obtained by arranging circular markings of diameter 0.2 μm on a flat surface is 22 μm^{-2}, which is nearly equal to the experimental value for v_p = 26%.

Interferometry on Crack-Tip Crazes

For v_p = 0.0026 and 0.026% the interference patterns (Fig. 4) are similar to those observed in pure PMMA[10,11,12]: They show fringes corresponding to the

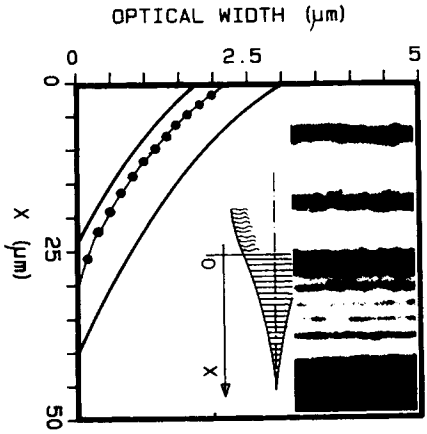

Fig. 4. Interference fringe pattern of a crack-tip craze for v_p = 0.0026%:(●) Corresponding profile calculated from the fringes on the photograph; (—) the range of profiles that can be observed in pure PMMA (data from Ref. 15).

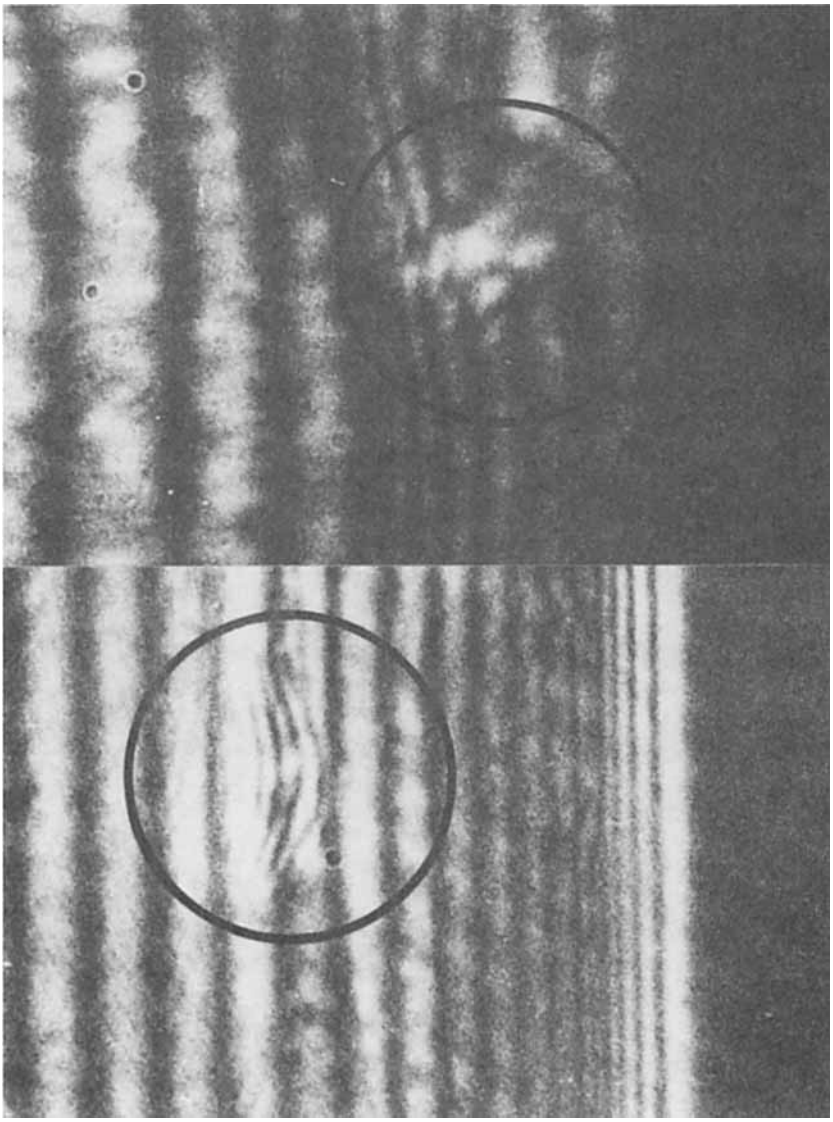

Fig. 5. Interference patterns for $v_p = 0.26\%$: (a) perturbation at the craze front; (b) out-of-plane fringes beside the craze.

crack with a single craze at its tip. The size and profile of the craze are the same as in pure PMMA.

For $v_p = 0.26\%$ the same kind of interference patterns are observed [Figs. 5(a) and 5(b)]. The craze still has the same size, yet it is no longer as regular as those in pure PMMA since superimposed out-of-plane fringes appear, possibly indicating branched crazes. Lateral observation of the specimens showed short fish-bone-like branches on the crack, and sometimes crack/craze bundles at the crack tip.

For $v_p = 2.6$ and 26% interference fringe patterns no longer exist (Fig. 6); Lateral observations showed highly branched and blunted crack tips.

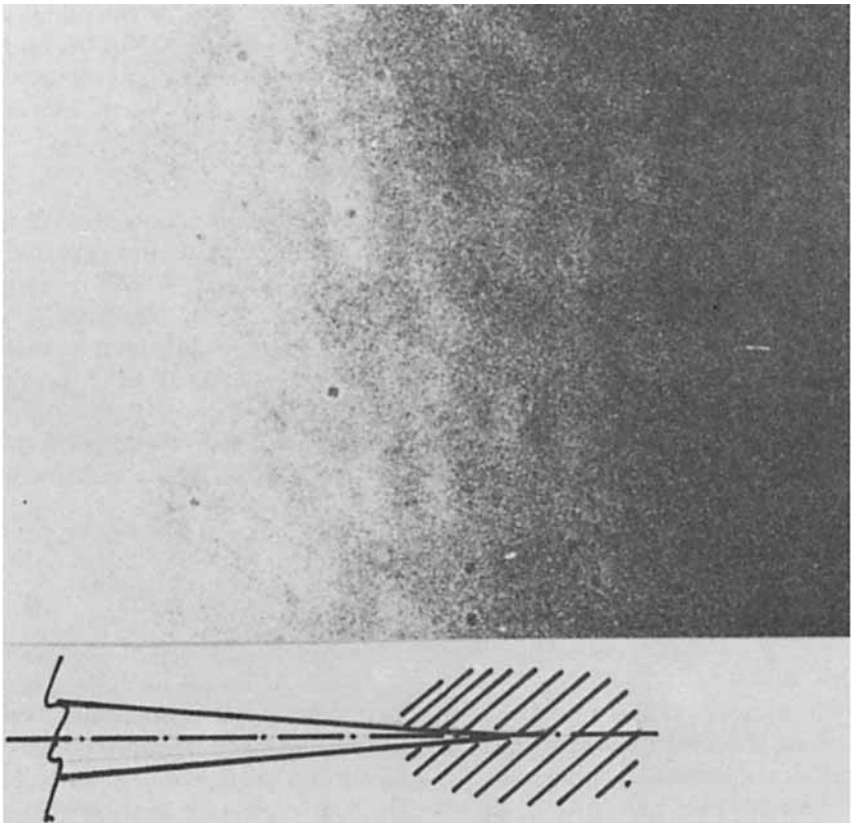

Fig. 6. Degeneration of the interference pattern for $v_p = 2.6\%$.

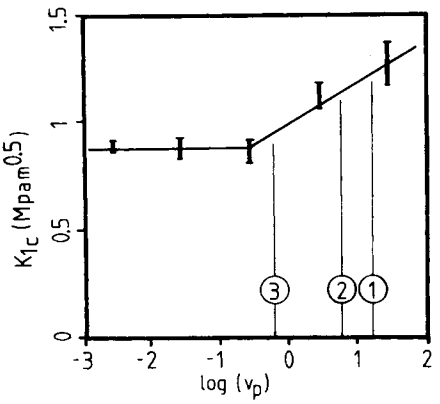

Fig. 7. Stress intensity factor at propagation K_{1c} (10μm/s) vs. the particle volume fraction. Thresholds for the onset of toughness: (1) Matsuo[7]; (2) Refs. 5 and 6; (3) actual experimental threshold.

Quantitative results are given as Φ_{INT} vs. v_p, where Φ_{INT} is the number of perturbations of the fringe pattern that are visible in the field F of the optical microscope ($F = 0.2$ mm^2). The experimental values of Φ_{INT} are reported in Table 1 and in Figure 3.

Toughness of Materials

The stress intensity factor K_{1c} was recorded during the steady-state propagations of the crack-tip crazes under static loading; results are reported in Table 1 and Figure 7. In the case of the material with $v_p = 26\%$, no proper steady-state propagation exists since extensive crack tip blunting occurs. Therefore, in this case K_{1c} was measured under static loading at the onset of the propagation of a sharp crack tip obtained by means of a previous propagation under 200 Hz fatigue loading.

In this material particle volume fractions below 0.26% have no effect on toughness, whereas for v_p above 2.6% the toughness increases with increasing v_p.

DISCUSSION

Material Toughness

This problem is classically treated by means of stress analysis. In the vicinity of each rubbery particle the stress field is enhanced, thus locally increasing the probability for initiation of damages like microshear bands or crazes. Since the stress enhancement attached to a particle decreases quickly with distance from the particle, the effect of overlapping stress enhancements does not exist for very low particle volume fractions, and increases with increasing v_p. The overlap of stress enhancement fields has two consequences: (i) at a given distance from a particle, the stress enhancement is increased; (ii) the size of the region concerned with stress enhancement near a particle is increased, which can allow craze initiation in a material containing only small particles.

Thus an efficient toughening can be achieved only with high enough particle volume fractions. Lower bounds for v_p can be found in the literature: Some are based on pure stress analysis[7,8,13]; others have been derived more pragmatically.[1,6] They are based on the evaluation of the maximum distance from a particle beyond which the stress enhancement is negligible ($A/R' = 2.9$, $v_p = 17\%$ for Matsuo et al.[7]; $A/R' = 3$, $v_p = 15.5\%$ for Oxborough and Bowden[8]; $A/R' = 4$, $v_p = 6.5\%$ for others as reported by Kinloch and Young or Bucknall[1,6]). The corresponding particle volume fractions for the onset of toughening have been reported as lines 1 and 2 in Figure 7 together with the K_{1c} measured at propagation. Clearly these limits are correct for practical use, but too high from a fundamental point of view, since they fall in a range where K_{1c} is 20–40% higher than for the matrix alone, and near the onset of high crack tip blunting.

In Figure 7 the true threshold for interactions can be estimated (line 3) as $v_p = 0.6\%$ ($A/R' = 9$). Goodier's equations[5] show that for this particular value of v_p the major stress enhancement factor is below 1.05 along half the length of the line joining two neighboring particles (Poisson's ratios $\nu_p = 0.495$

for the particle, $\nu_m = 0.3$ for the matrix, ratio of bulk moduli K_p/K_m about 1); thus it is doubtful that the onset of the increase of toughness is due to overlapping stress fields.

SEM and Optical Interferometry

Increasing the particle volume fraction leads to modifications in toughness, crack tip morphology, and aspects of the fracture surfaces. The fact that particles interact via their stress fields would be a sufficient reason for the crack tip morphology to change. However, we have just seen that stress analysis does not account satisfactorily for the onset of the increase of toughness; moreover, a noticeable amount of perturbations of the fringe pattern can be seen for v_p as low as 0.26% (Fig. 5), i.e., even below the lowest bound for the onset of toughness found in the previous section (0.6%); thus there is another kind of interaction between particles.

Additionally, as Figure 3 shows, one single mechanism cannot account for both optical interference and SEM results. The calculations below will show that SEM observations are consistent with mechanisms involving one particle, and interferometry results with two-particle mechanisms.

Crack-Tip Craze Propagation

The interference pattern experiments have shown that the crack-tip craze propagates in a steady state way for PMMAs with up to 0.26% particle volume fractions.

Now, it has been shown that a steady state propagating crack-tip craze generally moves by drawing fibrils out of the bulk. The craze surface stress profile is almost constant along the craze with a little dependence on the drawing speed. The most commonly admitted picture of the steady state propagation of a crack-tip craze in PMMA is the following[14,15]: (i) transformation of a "craze precursor zone" which is a layer of bulk PMMA (thickness $h = 1$ μm) into fibrils; (ii) breakdown of the fibrils at the back side of the craze and propagation of the crack into the craze.

Statistical Model for the Distribution of Particles in the Material

The craze precursor zone is schematically represented in Figure 8. Considering a surface $dS = dx \cdot dy$ of the craze plane, the corresponding volume of

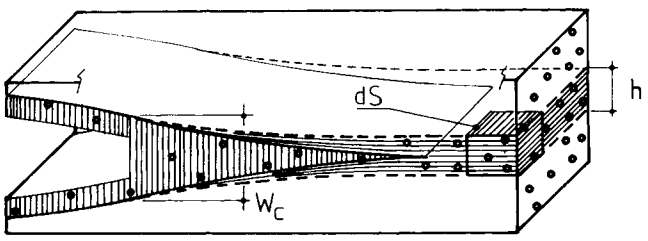

Fig. 8. Drawing showing the wedge-shaped crack-tip craze with the vertical fibrils and the "craze precursor zone" ahead of the craze.

material to be transformed into craze matter is

$$dV = h\,dS = h\,dx dy \tag{5}$$

and it contains a number dN_1 of particles that are distributed at random:

$$dN_1 = N_0\,dV = N_0 h\,dS \tag{6}$$

SEM

As mentioned in the first subsection of results, experiments show that the density of markings on the fracture surface (ρ_{SEM}) is proportional to the particle volume fraction v_p, thus to the number of particles per unit volume.

Assuming that every particle initially present in the "craze precursor zone" leaves a marking on the fracture surface yields a calculated density:

$$\rho_1 = dN_1/dS = N_0 h \tag{7}$$

Values of ρ_1 (in μm^{-2}) calculated for $h = 1$ μm and $R' = 0.12$ μm are reported in Table 1 and plotted in Figure 3 as a solid line that fits the experimental results for ρ_{SEM}.

A question that remains open is what is the mechanism through which markings form. Immediate breakdown or debonding of the particles under the enhanced stress field near the craze would not be consistent with the existence of interactions between particles. Moreover, unlike in HIPS [Figs. 9(a) and 9(b)], debonded or torn particles have never been found in the markings even at very high magnifications. An alternate explanation is that particles absorbed by the craze do not disturb the failing mechanism of the fibrils, which break after a characteristic lifetime[15] and form a partially relaxed layer behind the craze. The thickness of the layer, measured by interferometry,[16] is 30–40% higher than the initial thickness of the corresponding layer of bulk. But if the layer contains an intact elastically retracted rubber particle which is still bonded to the matrix, a hollow of some 0.1 μm depth and 0.2 μm diameter will appear at the surface.

Optical Interferometry

As can be seen in Figure 3, the exponent in the scaling law for the density of perturbations of the fringe pattern vs. the particle volume fraction is more than 1, which indicates a mechanism involving interactions between particles.

Such a mechanism may consist of a geometrical "sifter" effect as described below.

The particles (about 0.2 μm diameter) are much smaller than the maximum craze thickness (2 μm), unlike in classical HIPS for example. On the other hand, they are much larger than the craze fibril diameter and interfibril spacing (both 0.02 μm) so that if a particle is absorbed by a craze without fibrillating it must bridge a great number of fibrils. Since the particles are well bonded to the matrix and do not contain rigid occlusions, they are not likely to fibrillate easily under the enhanced stress at the craze tip: Rather, the craze will deviate into the surrounding matrix.[17] However, as the slightly

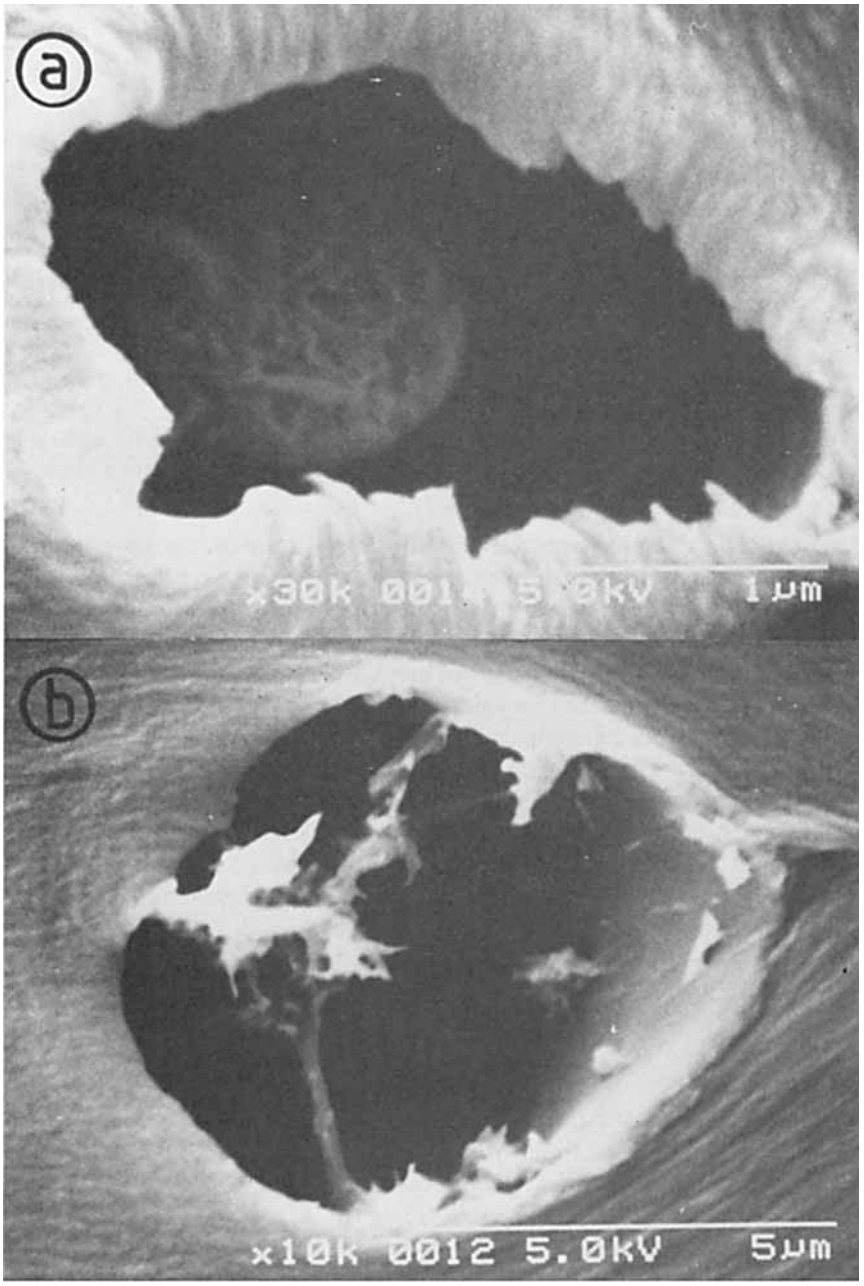

Fig. 9. Markings on fracture surfaces of HIPS in which particles are visible: (a) debonded particle; (b) torn particle.

deviated craze advances, it thickens by incorporating the layer of PMMA in which the particle is embedded.

If no material can be drawn out of the crosslinked particle, the fibril drawing process at the particle/craze interface is stopped. But as long as no other particle appears at the opposite craze/bulk interface, the process can

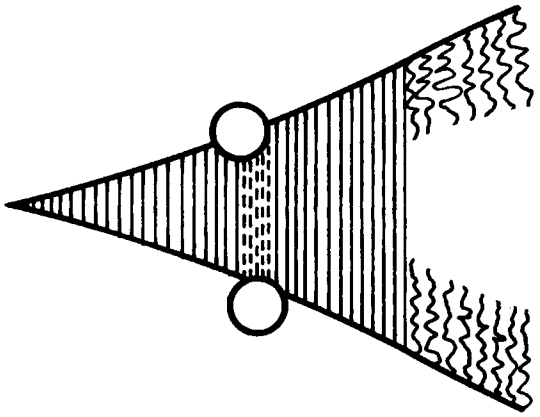

Fig. 10. Geometrical "sifter" effect when a propagating craze of thickness W_c slips between two particles distant from $S < h$ (S is the edge-to-edge distance in the undeformed material).

still take place at the other end of the fibrils, with a drawing speed twice as high and no noticeable change in craze stress.

Conversely, if two particles are face to face on the opposite craze surfaces, the fibril drawing process can take place at neither fibril end (Fig 10) and some other mechanism must occur, such as breakdown of fibrils between the two particles, initiation of a secondary craze in the bulk, or branching of the main craze. These latter mechanisms could account for the aspect of the perturbations that are observed, unlike particle breakdown or debonding occuring either when the craze meets a single particle or when the fibril drawing process is inhibited.

The theoretical density ρ_2 of perturbations of the interference fringe pattern will be given by the number of cases where, in the "craze precursor zone," two particles have positions that are symmetric with respect to the craze plane.

The probability for such an event is zero if we demand a perfect symmetry of positions. Of course, this is not the case since the effect can still arise when the position of the second particle is shifted of $\Delta \leq R'$ from the perfectly symmetric case.

Consider a particle #1 in the lower half part of the zone $dV = h \cdot dS$, for instance. The positions of the center of a particle #2 in the upper half zone that will allow an interaction are those inside a sphere of radius Δ around the perfectly symmetric position (Fig. 11). Thus the probability for the particles #1 and #2 to interact is equal to the volume of the sphere divided by that of the half zone:

$$p_{12} = (4\pi\Delta^3/3)(h\,dS/2)^{-1} \tag{8}$$

Since the zone dV contains dN_1 particles (so each half of it contains $dN_1/2$), the theoretical number of interactions on the surface dS is

$$\rho_2\,dS = p_{12}(dN_1/2)(dN_1/2) \tag{9}$$

Thus the theoretical number of perturbations in the field F of the optical

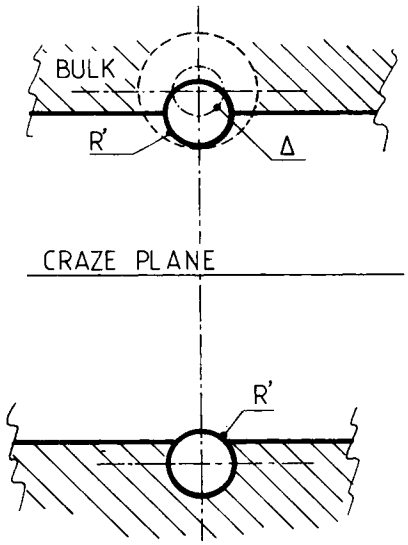

Fig. 11. Geometrical requirement for the sifter effect to occur: the center of the particle #2 must be inside the sphere of radius Δ (the positions of the centers of the sphere and of the particle #1 are exactly symmetric with respect to the craze plane). The ratio Δ/R' is between 0 and 1.

microscope is

$$\Phi_2 = 2\pi h \Delta^3 N_0^2 F/3 \tag{10}$$

Calculated values of Φ_2 (for $h = 1$ μm, $R' = 0.12$ μm and $\Delta/R' = 0.35$) are reported in Table 1, where it can be seen that the agreement with the experimental values (Φ_{INT}) is very good. The choice of the symmetry misfit Δ is somewhat arbitrary. However, in the first place changing Δ does not change the slope of $\log(\Phi_2)$ vs. $\log(v_p)$, and moreover, in our case, any value of Δ/R' between 0.2 and 0.4 yields values of Φ_2 that agree with experiment, which seems reasonable. A slight deviation from the direction normal to the craze plane is allowed for the extraction of the fibrils (because there are cross-tie fibrils), so when the distance between particles is as much as 5 times their diameter, inhibition of the extraction process is not likely to occur for shifts Δ that are equal or close to R'.

Quite a similar situation has been reported by Wu[18] for the sharp fragile/ductile transition in notched impact tests on rubber toughened PA 66. He found a critical interparticle distance of 0.3 μm independent of particle volume fraction and size. In this case too the transition was probably associated with the relative values of interparticle distance and thickness of crazes such as those observed by Lee et al.[19]

CONCLUSIONS

1. The crack-tip craze is able to absorb small particles.
2. For any particle volume fraction, each particle absorbed by the crack-tip craze leaves a marking on the fracture surface (markings can be seen by means of SEM).

3. An isolated small rubber particle does not induce any perturbation on the optical interference pattern of a propagating crack-tip craze.

4. In this material containing small rubber particles, the increase of toughness arises through two mechanisms, both of which involve interactions between particles:

— A geometrical "sifter" effect which occurs when the craze has not enough room to slip between two particles that locally inhibit the fibril extraction process. The corresponding increase of toughness is associated with a transition from a single craze to a bundle of crazes, which takes place when the particle volume fraction v_p increases from 0.6 to 3% (in other words the ratio $\langle A \rangle / R'$ decreases from 9 to 5).
— The well-known overlap of stress field enhancements of particles, which occurs when v_p is above 6–17% (i.e., $\langle A \rangle / R'$ is less than 4–3) and which is associated with an additional increase of the size of the zone where damage occurs at the crack tip.

5. From an engineering point of view, a noticeable increase in material toughness is obtained only for the particle volume fractions above ca. 10%, in agreement with literature values.

This work was performed at the Institut Charles Sadron, Strasbourg (France) and supported by the company NORSOLOR SA under Grant No. 86-22. Also we thank Professor C. Wippler for helpful discussion and Dr. D. Lefebvre from NORSOLOR for having supplied the materials.

References

1. A. J. Kinloch and R. J. Young in *Fracture Behavior of Polymers*, Applied Science, London, 1983, Chaps. 5 and 11.
2. H. Breuer, F. Haaf and J. Stabenow, *J. Macromol. Sci. Phys.*, **B14**(3), 387 (1977).
3. A. M. Donald and E. J. Kramer, *J. Mater. Sci*, **17**, 1765 (1982).
4. J. Silberberg and C. D. Han, *J. Appl. Polym. Sci.* **22**, 599 (1978).
5. J. N. Goodier, *J. Appl. Mech.*, **55**, 39 (1933).
6. C. B. Bucknall, in *Toughened Plastics*, Applied Science, London, 1977, Chap. 5.
7. M. Matsuo, T. Wang, and T. K Kwei, *J. Polym. Sci.*, A-2, **10**, 1085 (1972).
8. R. J. Oxborough and P. B. Bowden, *Phil. Mag.* **30**, 171 (1974).
9. A. M. Donald and E. J. Kramer, *J. Appl. Polym. Sci.*, **27**(10), 3729 (1982).
10. W. Doll, *Adv. Polym. Sci.*, **52 / 53**, 105 (1983).
11. R. Schirrer and C. Goett, *J. Mater. Sci.*, **16**, 2563 (1981).
12. K. Jud, H. H. Kausch, and J. G. Williams, *J. Mater. Sci.*, **16**, 204 (1981).
13. L. J. Broutman and G. Panizza, *Int. J. Polym. Mater.*, **1**, 95 (1971).
14. E. J. Kramer, *Adv. Polym. Sci.*, **52 / 53**, 1 (1983).
15. P. Trassaert and R. Schirrer, *J. Mater. Sci.*, **18**, 3004 (1983).
16. R. P. Kambour, *J. Polym. Sci.* **A3**, 1713 (1965).
17. R. P. Burford and M. Pittolo, *J. Mater. Sci. Lett.*, **6**, 969 (1987).
18. S. Wu, *Polymer*, **26**, 1855 (1985).
19. L. H. Lee, J. F. Mandell and F. J. McGarry, *Polym. Eng. Sci.*, **27**(15), 1128 (1987).

Received February 24, 1989
Accepted April 10, 1989